

# PRECISE MEASUREMENT OF PROPAGATING FLAME IN 2-STROKE GASOLINE ENGINE BY MULTIPLE ION-PROBES

Tomoaki Yatsufusa\*, Keigo Kii\*, Kentaro Takatani\*  
\*Hiroshima Institute of Technology

## Abstract

*Multiple ion-probes method is the measurement method of propagating flame by multiple ion-probes installed tow-dimensionally on the confined chamber wall surface. Previous studies adopted this method to well controlled various propagating flames in constant volume combustion tube to investigate the characteristics of measurement, and found that this method provides fine measurement results on such flames. This study aimed to capture the propagating flame in piston gasoline engines by multiple ion-probes as a first step for precise measurement on destructive combustion in piston engine called “knocking”.*

## 1 Introduction

Detailed measurement of combustion in piston gasoline engine is inherently difficult because of its high temperature and impulsive high pressure caused by high-intensity and explosive combustion [1,2]. In general, combustion in engines is often investigated by visualization and pressure measurement.

The visualization-technique inside a reciprocating piston engine generally utilizes optically-accessible transparent window [3,4] at engine development in laboratories [5-9] and manufactures [10,11]. However, observation window generally made of tempered glass does not have enough strength especially for impulsive high pressure occurred in piston engines even if such strong and expensive materials are chosen. Therefore, operational conditions of engines with optical windows is generally forced to be limited in low-load conditions.

Pressure measurement in cylinder is also widely used to investigate the state of combustion. Compare to the optical investigation, pressure sensor is much stronger, but it can only capture indirect information of combustion.

On the contrary, ion-probe method detects the flame using electric conductivity of the flame. Chemical reaction zone in combustion field has usually ionized intermediate products which is electrically conductive. Once the flame contacts the ion-probe electrically charged, ion-current flows between the ion-probe and ground via chemical reaction zone. By measuring the ion-current, it is able to estimate not only the existence of the flame but also the strength of the chemical reaction can be estimated. Because this simple principle to detect makes this method inexpensive and physically strong, this method is often used in measurement of explosive combustion in experimental field.

However, this ion-probe method can only detect the existence of the flame and estimate the strength of the chemical reaction at a certain point where the tip of the ion-probe. In other words, independent single ion-probe cannot provide the spatial information of propagating flame.

Newly developed ion-probe method using multiple ion-probes installed densely on the confinement chamber wall by our group provides one solution discussed above. Multiple ion-probes detect the flame one by one as flame propagating. If the installation of ion-probes is dense and large number, temporal and spatial behavior of the flame propagation along the chamber wall can be reproduced by recorded ion-probe signals detected by each ion-probe.

In the previous studies [12-14], performance of the multi ion-probes method has

been investigated by using the propagating flame of LPG-oxygen-nitrogen mixture in confined tube. Combustible mixture was made by mixing the stoichiometric LPG-oxygen and nitrogen as diluent to vary widely the combustion characteristics. Largest diluent, which simulates the mixture of stoichiometric LPG-air, provides the flame propagation speed of a several meter per second. No dilution case provides fully developed detonation propagating at the speed of about 2.3km/s, which is twice faster than general flame propagation under knocking condition in reciprocating spark ignition engines. Multiple ion-probes method can capture the details of the flame propagation in both extreme conditions.

## 2 Experimental setup

Fig. 1 shows the schematics of the multiple ion-probe measurement system. The system mainly consists of multiple ion-probes, signal amplification circuit, data acquisition system and post data processing system. The figure also shows photographic image of the measurement system and tested 2-stroke gasoline engine.

In the present study, air-cooled 2-stroke gasoline engine has been selected because the simplicity of the cylinder head geometry makes it easy to install the ion-probes. The details of the engine are listed in table 2. Although the

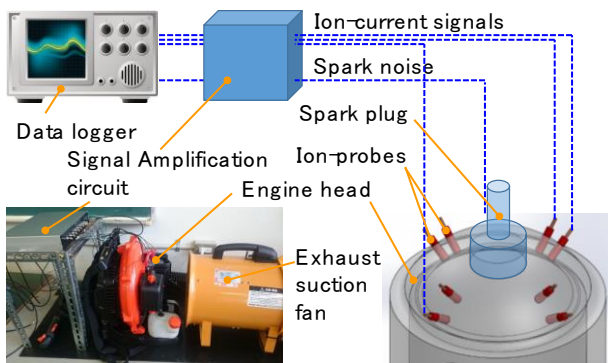


Fig. 1 Overview of measurement system

Table 1 Details of experimental 2-stroke gasoline engine

Engine type	Single cylinder air-cooled 2-stroke gasoline engine
Displacement	58.2cc
Equipped product	Power blower

experimental engine was modified with installation of ion-probes, the engine can run by itself. 2-stroke gasoline engine with the displacement of 58.2cc on power blower was used. The engine always runs with load by blower fan connected with engine output shaft.

Outward appearance of the engine ion-probes installed is shown in fig. 2. Details of ion-probe installation is illustrated in fig.3. Eight ion-probes are installed. Each ion-probe is defined by coordination of  $\phi$  for longitudinal direction and  $\theta$  for latitudinal direction.

In the previous studies, signals from multiple ion-probes was recorded by originally developed data acquisition system based on

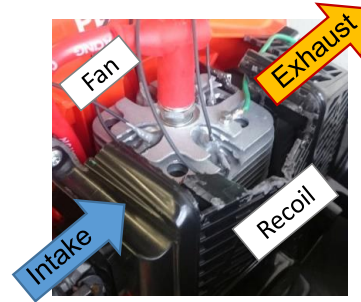


Fig. 2 Installation of ion-probes on engine head

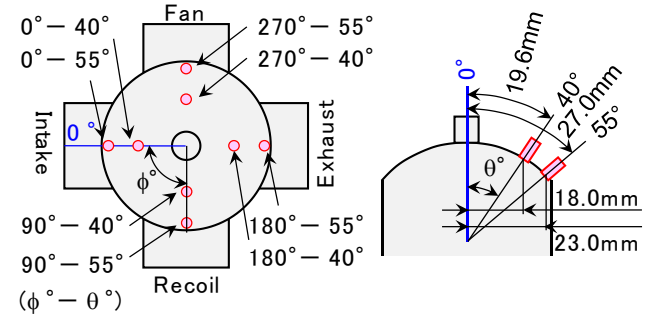


Fig. 3 Notation of ion-probe position on engine head

Table 2 List of recorded ion-probes in each experiment

Ex. No.	CH 1 (Spark)	CH 2 (P-1)	CH 3 (P-2)	CH 4 (P-3)
1	Spark plug	270°-40°	180°-40°	90°-40°
2	Spark plug	270°-40°	0°-40°	90°-40°
3	Spark plug	270°-55°	180°-55°	90°-55°
4	Spark plug	270°-55°	0°-55°	90°-55°
5	Spark plug	0°-40°	180°-40°	180°-55°
6	Spark plug	0°-55°	0°-40°	180°-40°
7	Spark plug	0°-55°	180°-40°	180°-55°
8	Spark plug	0°-55°	0°-40°	180°-55°

FPGA, which is able to record 64 channels simultaneously [14]. On the contrary, the present study uses the data logger with four recordable channels only because longer recording duration is required. In addition, one of four channels was used to record the spark noise signal to detect the spark timing. Therefore, only three ion-probe signals were recorded in single experiment.

Totally eight experiments were conducted by changing the recording ion-probe as shown in table 2. Details of recorded ion-probes configuration were shown in fig. 3.

This study aims to get statistical information of ion-signal from multi cycles in longer duration of engine operation rather than

details of a certain single operating cycle. Therefore, slower data sampling rate of 10kS/s and longer recording duration of a few tens of seconds were selected for data recording. Total number of recoded data words was up to a few millions. Post data processing was conducted by Microsoft Excel VBA, IGOR and ParaView.

### 3 Results and discussions

#### 3.1 Characteristics of ion-probe signals

In the beginning of experiment, engine was warmed up by 10 minutes of running with IDLE operation. After warming up, several times of

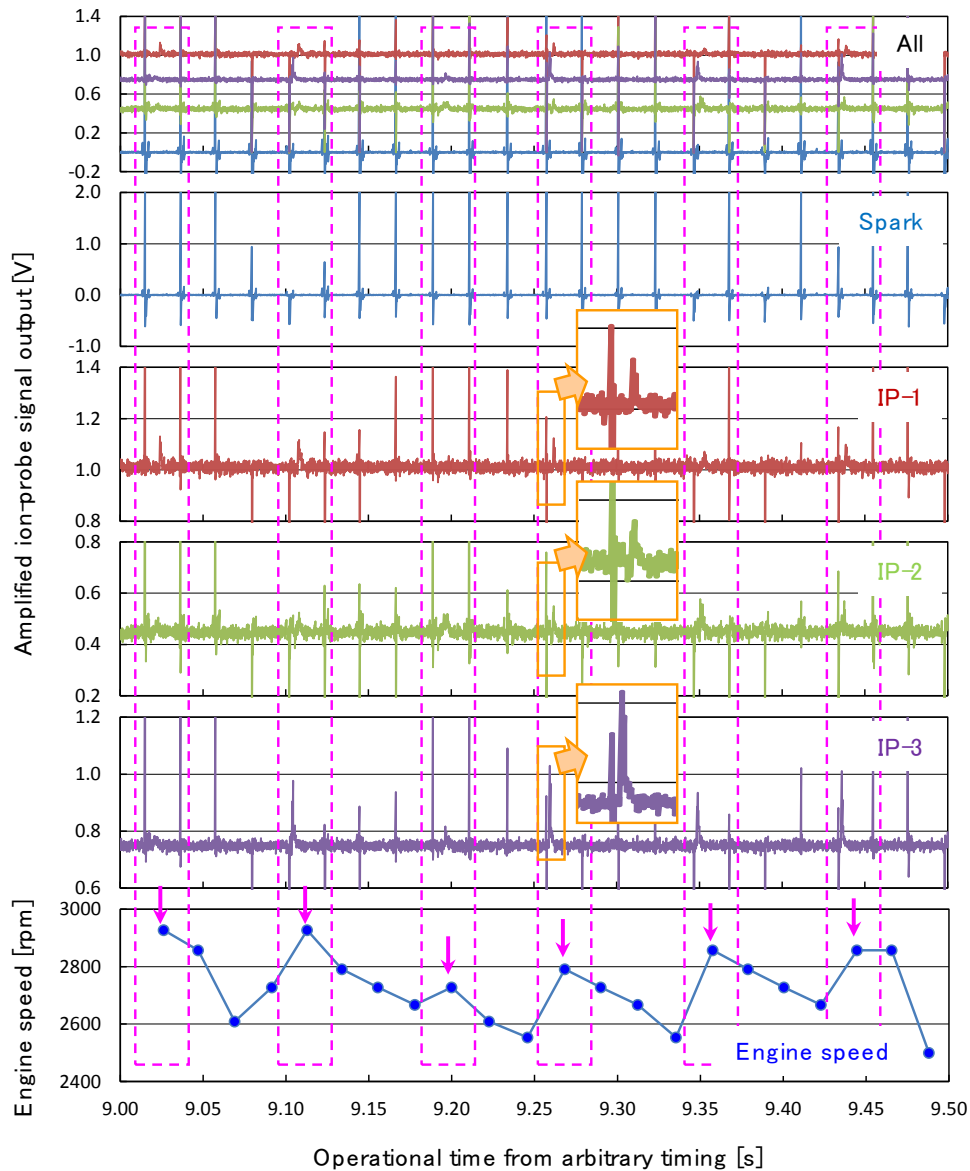


Fig. 4. Raw ion-signal waveforms in IDLE operating condition (Ex. No.6)

experiments were continuously executed. Engine operation procedures under recording operation consisted of initial 10 seconds of IDLE, following 10 seconds operation of WOT (Wide Open Throttle) after initial IDLE, and additional IDLE operation with a few tens of second for cooling down the engine. Total engine operation durations with recording were 60-100 seconds.

Fig. 4 and fig. 5 show one example of obtained signals in IDLE and WOT operation respectively. These signals were obtained from experiment No.6 shown in table 2. Detailed discussion of the signals in the present paper will be done by mainly using this data. Both of the fig. 4 and fig. 5 have uppermost row of combined all

signals from four channels, second row of the signal from spark noise and the third to fifth rows of amplified ion-probe signals from IP-1( $0^{\circ}$ - $55^{\circ}$ ), IP-2( $0^{\circ}$ - $40^{\circ}$ ) and IP-3( $180^{\circ}$ - $40^{\circ}$ ) respectively. Lowermost row is the calculated engine speed of respective cycle by interval of spark signal.

Fig. 4 extracts a certain 0.5 second from initial IDLE operation. In the extracted duration of 0.5 seconds, 23 times of spark noise are observed in spark noise signal. This means that average engine speed was 2760rpm, which roughly corresponds to the value measured by speed indicator simultaneously. Cycle to cycle engine speed fluctuates every three to four cycles. The cycles with higher engine speed than

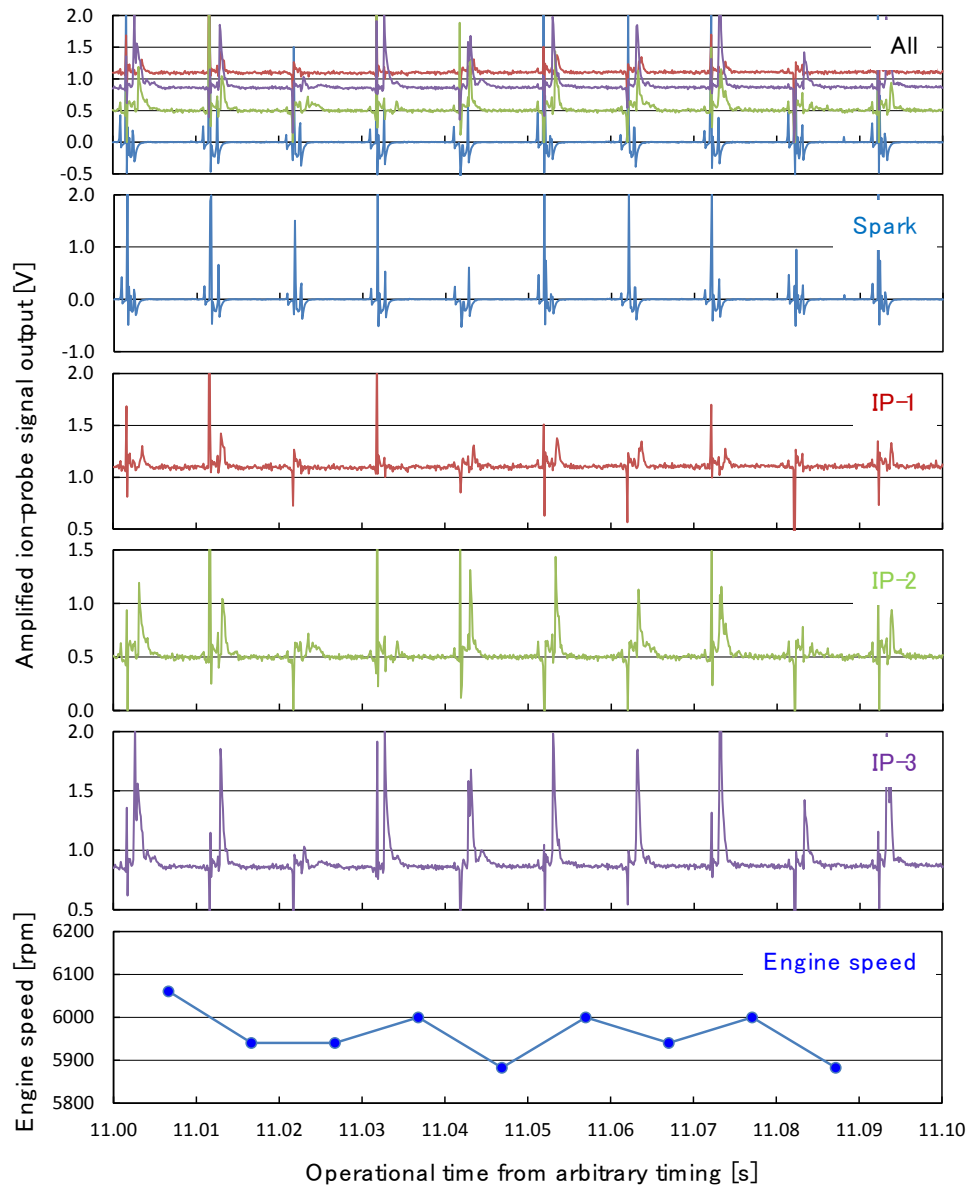


Fig. 5. Raw ion-signal waveforms in WOT operating condition (Ex. No.6)



neighbor cycles are resulted by firing. These fired cycles are indicated by arrows and surrounded by dotted square. On the contrary, the cycles with lower engine speed are caused by miss-firing. This repetition of fired and miss-fired cycle is basic characteristic of Day type 2-stroke gasoline engine on IDLE operation. The overall span of vertical axis in the third to fifth row showing IP-1 to IP3 is 0.6V. The 4th fired cycle in displayed duration in fig. 4 is enlarged in the figure. 4th fired cycle in IP-3 shows initial spark noise and the following flame signal. Flame signal includes initial sharp rise and relatively gentle descent. Even in IP-1 and IP-2, small flame signals, which are not strong as IP-3, are observed in 4th fired cycle. Although the flame signals are observed in other fired cycle, strength of the signals are different from cycle to cycle. In addition, signals in IP-1 and IP-2 tend to be weaker than that of IP-3. Highest signal peak by flame is about 0.1V in IP-1, 0.1V in IP-2, and 0.2V in IP-3 respectively. Possible reasons cause the difference of signal strength in each cycle are cycle to cycle fluctuation of combustion including strength of combustion, and so on. Compare to the fired cycle, there are no signal peak except park noise in miss-fired cycle. Therefore, these facts indicate that the signal peak in fired cycle is surely caused by flame contact to the ion-probe.

Recorded signals in WOT operation of No.6 experiment is shown in fig. 5. In contrast to IDLE operational operation, all cycles shown in the figure were fired in WOT operation. The fluctuation of engine speed shown in lowermost row is less than that of IDLE operation shown in fig. 4. The overall span of vertical axis in the third

to fifth row is 1.5V. Overall horizontal span of the figure is 0.1 second, which is one fifth of fig. 4. IP-3 signal shows strong flame signal in any cycles. Highest peak of flame signal is about 1.0V that is about five times higher than that of IDLE operations. Strength of flame signal in IP-1 and IP-2 tend to be weaker than that of IP-3. This tendency is same as in IDLE operation. In spite of stable ignition in WOT operation, strength or height of flame-signal peak fluctuates from cycle to cycle. This must be resulted by cycle to cycle fluctuation of combustion.

### 3.2 Flame signal extraction and indirect visualization of propagating flame

As mentioned above, strength of flame signal varies as changing the operating condition and different ion-probes. Therefore, threshold value to extract the flame signal should be changed as operating condition and each ion-probe.

Example of the results on flame signal extraction from experiment No.6 is shown in fig. 6. Extracted signals are shown as time difference between spark ignition and flame detection time. In other words, vertical axis of the figure is the duration of flame propagation from spark plug to individual ion-probes. This figure also shows cycle interval indicated by x mark, which is inversely proportional to engine speed. Initial 10 seconds is IDLE operation and following 10 seconds is WOT operation. Engine speed measured by speed indicator beside simultaneously is about 3000rpm and 6000rpm in IDLE and WOT operation respectively. Measured cycle interval mostly corresponds to these speed. Spark timing is identified using

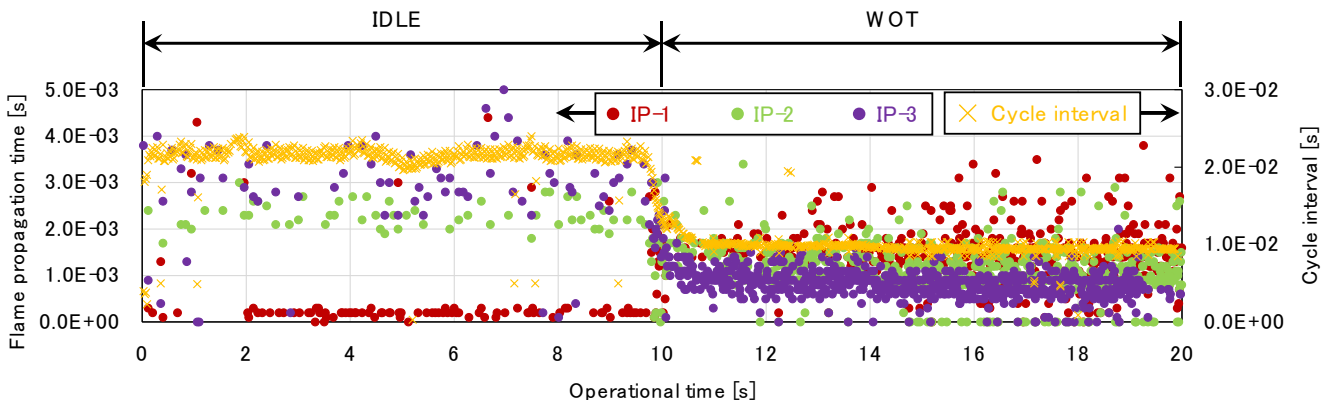


Fig. 6. Flame propagation duration in IDLE and WOT operating conditions (Ex. No.6)

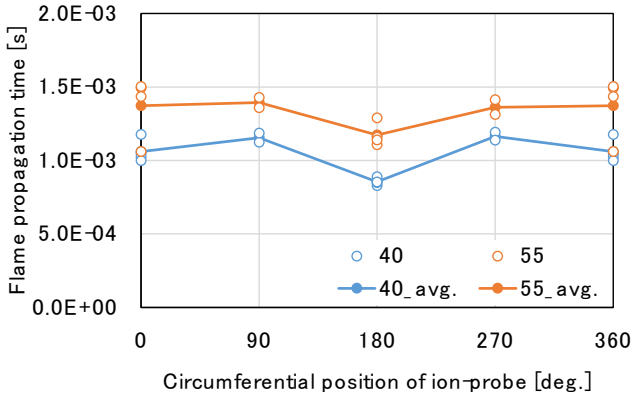


Fig. 7 About 1,000 cycles averaged flame propagation duration at each ion-probe

spark signal for example shown in second row in fig. 4 and 5. Spark signal includes initial positive spike and immediately following second negative spike. Time interval between initial positive peak and second negative peak is about  $1.0 \times 10^{-4}$  seconds. Because secondary negative spike is more stable than positive spike, second spike is defined as spark timing. Flame signal is automatically detected by searching the peak larger than appropriate threshold voltage just after the spark timing. The value of threshold voltage is adjusted for each ion-probe. Error elimination is not performed.

In IDLE operation of initial 10 seconds, many data points indicated by red mark of IP-1 have the value of about  $0.2 \times 10^{-3}$  seconds and are considerably smaller value than others. These must be error on flame signal extraction. This is mainly caused by low threshold voltage for extraction. Excluding these points, most data points in IP-1 that is on intake side are in the range of 3.0-4.0ms, which corresponds to 7-9m/s in the distance of 27mm between spark plug and ion-probe along to wall. In case of IP-2 that is on intake side, data points are in 2.0-3.0ms, which corresponds to 7-10m/s in the distance of 19.6mm. In IP-3 that is exhaust side, data points are in 2.5-4.0ms, which corresponds to 5-8m/s in the distance of 19.6mm.

In WOT operation, the number of detected flame is considerably larger than IDLE operation. This is caused by both of higher firing rate and larger signal peak than IDLE operation for reliable signal extraction. Flame propagation time in WOT operation is less than that in IDLE operation. In the present case, IP-1 is in the range of around 0.5-3.0ms, which corresponds to 9-54m/s. IP-2 and IP-3 are 0.5-2.0ms and 0.5-1.5ms, which corresponds to 10-39m/s and 13-39m/s respectively. These are obviously faster than that in IDLE operation. Propagating flame velocity generally increases as increase in engine

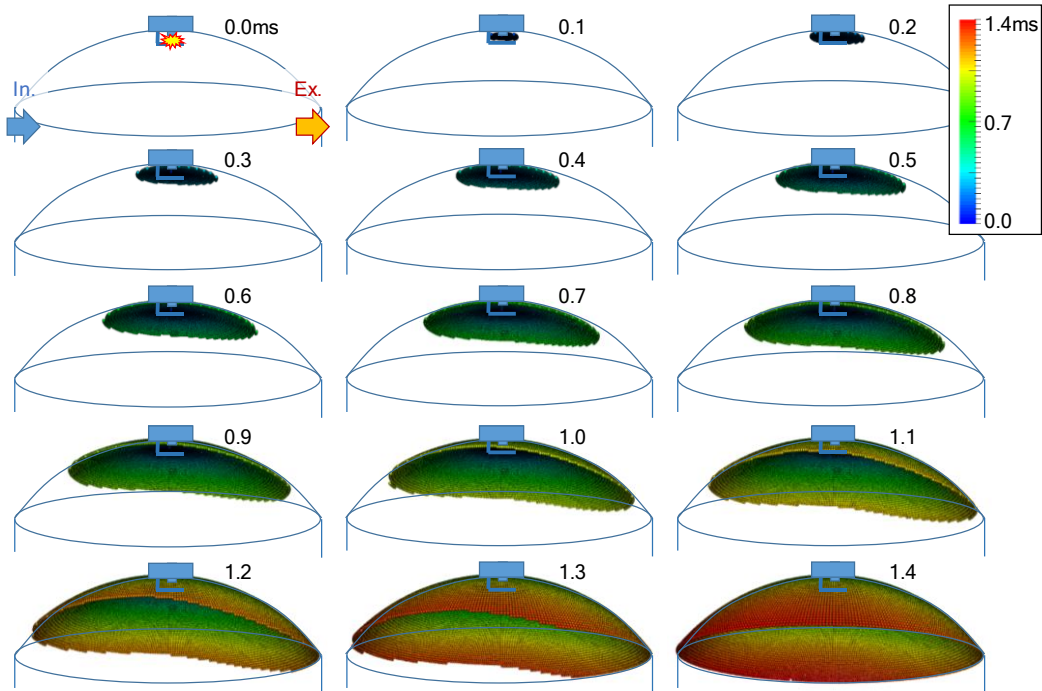


Fig. 8 Re-generated animation of flame propagation behavior in 2-stroke gasoline engine

speed, because increase in engine speed results stronger turbulent enhances flame propagation. Increase in flame propagation velocity according to increased engine speed observed in this experiment does not contradict the generally known feature in engine combustion. Therefore, extracted signal is surely the signal from propagating flame.

Average value of flame propagation duration in WOT was calculated and shown in fig. 7. All data obtained from plural experiments listed in table 2 were used to calculate these average and standard deviation. On the other hand, this procedure was not adopted for IDLE because the number of extracted flame signals is not large enough. In this experiment, WOT operation was 10 seconds, which includes about a thousand engine cycles. Therefore, fig. 7 shows average characteristics of about a thousand engine cycles. In this data processing, outside data from 0.1-1.9 times of initial average value on original data were eliminated as error data. The group of data eliminated the error was averaged again to get averaged value of flame propagation duration.

Orange and blue data indicate  $\theta^\circ = 40^\circ$  and  $55^\circ$  respectively from spark plug as defined in fig. 7. In fig. 7, averaged flame propagation time in both of  $\theta^\circ = 40^\circ$  and  $55^\circ$  shows shortest value in circumferential position of  $180^\circ$ . This direction corresponds to the exhaust port. Average propagation time in another direction does not have significant difference. It is conceivable that flame propagating toward the exhaust port is accelerated by induced flow in scavenging process.

Temporal and spatial behavior of flame propagation is able to be re-generated as animation by averaged value of flame propagation time. Reference data points are eight ion-probes and spark plug, where the origin of flame propagation. Averaged flame detection time at the ion-probes shown in fig. 7 are used to generate the animation. Flame propagation time between these nine points was interpolated by cubic spline method. This bold interpolation is valid to a certain degree, because the values of reference data points are already heavily averaged and the change of value between adjacent data points is relatively smooth.

Fig. 8 shows re-generated animation of flame propagation behavior. This can also be called as “indirect visualization” of flame propagation inside the piston engine. Flame propagates faster in exhaust port direction than intake port direction. This is comprehensible because global flow inside the engine is from intake to exhaust port and propagating flame carried by this flow. In the present moment, Averaged flame behavior can only be re-generated. Re-generation of flame propagation in each cycle is now working in progress.

### 3.3 Sensitivity of flame detection

As mentioned before, threshold value to extract the flame signal should be varied by operating condition and each ion-probe. Fig. 9 shows

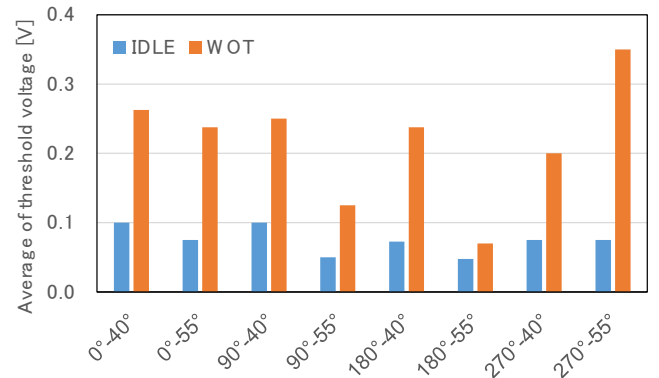


Fig. 9 Threshold voltage for extraction of flame signals

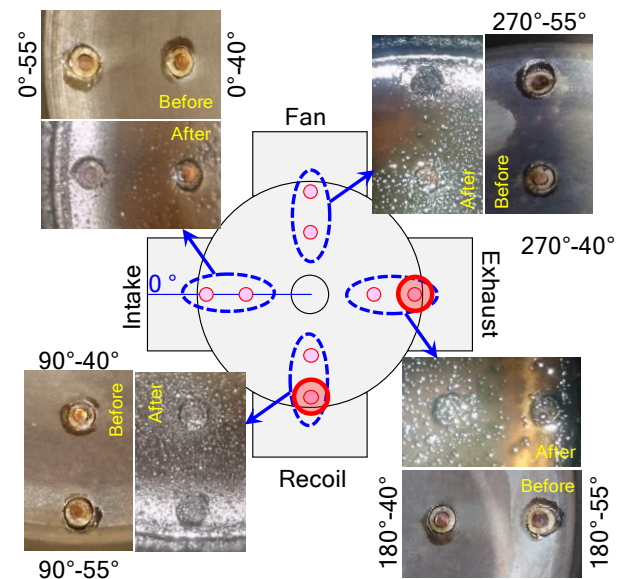


Fig. 10 Degree of pollution on ion-probes after 10 hours engine operation

average voltage of threshold value to extract the flame signal as shown in fig. 7. Lager threshold voltage tends to higher flame signal, and vice versa.

Threshold voltage in WOT is higher than that in IDLE. This is resulted by higher peak voltage of flame signal in WOT. In WOT, difference of threshold among the different ion-probes is significant. This is caused by individual difference of ion-probes. For example, threshold voltage of ion-probe 180°-55° is the shortest in WOT. This means that ion-probe 180°-55° is the most inactive ion-probe in WOT. On the contrary, 270°-55° is most reactive. In IDLE, the value of threshold less varies compare to that of WOT. However, ion-probe with lower threshold in WOT seems to have lower threshold in IDLE as well.

Fig. 10 is the photographic images of ion-probes before and after engine operation. Total engine operation duration is about 10 hours to overhaul and photographing these images. Red circled ion-probes are relatively inactive for detecting the flame signal. By comparing the images of after operation, exhaust side is heavily polluted by engine oil. At the present moment, the pollution of ion-probe surface by engine oil is one of the possibility to inactivate for capturing the ion-signal.

## 4 Conclusions

Measurement of propagating flame in 2-stroke gasoline engine by multiple ion-probes has been conducted.

In IDLE operation, firing and miss-firing cycle was able to be distinguished only by obtained ion-probe signals. In WOT (Wide Open Throttle) operation, relatively obvious flame signals were obtained.

Obtained large number of flame propagation data in WOT operation were statistically processed and averaged flame behavior was successfully re-generated as animation.

The sensitivity of flame detection by ion-probe in 2-stroke gasoline engine is affected by the pollution of ion-probe surface by engine oil.

## References

- [1] Ohta Y, Takahashi H, Prog. Astronaut Aeronaut, Vol.105, No.1, pp.69-77, (1986).
- [2] Hayashi T, Taki M, Kojima S, Kondo T, Compression and Expansion Machine, SAE Technical Paper 841336, (1984).
- [3] Merker G.P, Schwarz C, Teichmann R, Springer, 2011, pp. 91-114.
- [4] Hiroyasu H, Miao H, Springer, 2004, pp. 91-114.
- [5] Yatsufusa T, Kidoguchi Y, Adam A, Gomi T, ILASS-Japan., vol. 18, no. 63, pp. 88-95, (2009).
- [6] Khalid A, Yatsufusa T, Miyamoto T, Kawakami J, et al., SAE Technical Paper, 20097018, (2009).
- [7] Aoyagi Y, Kunishima E, Asaumi Y, Aihara Y, et al., JSME International Journal, Series B, vol.48, no.4, pp.648-655, (2005).
- [8] Wolanski P, Gut Z, Niedziela W, Przastek J, et al., SAE Technical Paper 972829, (1997).
- [9] Espey C, and Dec J, SAE Technical Paper 930971, (1993).
- [10] Fuyuto T, Akihama K, Fujikawa T, Nakakita K, Transactions of the Japan Society of Mechanical Engineers, Series B, vol. 74, no. 740, pp. 980-985, (2008).
- [11] Kuwahara K, Ando H, 4th international symposium for combustion diagnostics, pp. 130-137, Baden-Baden, May 18-19, (2000).
- [12] Yatsufusa T, Miyata S, Ishibashi K, Small Engine Technology Conference, JSAE 20159728 / SAE 2015-32-0728, (2015).
- [13] Yatsufusa T, Takatani K, Miyata S, 30th Congress of the International Council of the Aeronautical Sciences, 2016\_0418, (2016).
- [14] Miyata S, Takatani K, Kii K, Yatsufusa T, Proceedings of the Fifty-Fourth Symposium (Japanese) on Combustion, A312, (2016).

## Acknowledgement

This work was supported by JSPS KAKENHI Grant Number JP16K06133.

## Copyright Statement

The authors confirm that they, and/or their company or organization, hold copyright on all of the original material included in this paper. The authors also confirm that they have obtained permission, from the copyright holder of any third party material included in this paper, to publish it as part of their paper. The authors confirm that they give permission, or have obtained permission from the copyright holder of this paper, for the publication and distribution of this paper as part of the ICAS proceedings or as individual off-prints from the proceedings.